



# Synthesis and study bromophenol blue dye adsorption efficiency of reduced graphene oxide produced by catalytic acid spray (CAS) method

Mahmoud Fathy<sup>1</sup> · Th. Abdel Moghny<sup>1</sup> · Mahmoud Ahmed Mousa<sup>2</sup> · O. H. Abdelraheem<sup>3</sup> · Abeer A. Emam<sup>4</sup>

Received: 1 May 2018 / Revised: 15 March 2019 / Accepted: 7 May 2019 / Published online: 14 November 2019  
© Australian Ceramic Society 2019

## Abstract

In this work, novel nanostructure reduced graphene oxide was prepared using catalytic acid spray (CAS) method in the existence of cobalt silicate nanoparticles. The structure, morphology, chemical composition, and crystalline phase of these products were systematically studied and characterized by a number of modern techniques like FTIR, transmission electron microscopy, X-ray diffraction, and Raman characterizations. The homogenous distribution of layered graphene sheets were observed from representative TEM images. XRD shows that interlayer spacing of our prepared RGO is to some extent higher than others RGO produced by other process. Hence, achieving proper designs of highly efficient, sustainable, and long-term reusable RGO is one of the environmentally crucial issues facing humanity. Here, we report the fabrication of mesoporous RGO. The mesoporous RGO exhibit high catalytic activity and fast removal of bromophenol blue dye from synthetic polluted water.

**Keywords** Graphene · Catalyst · Spray · Interspacing · Lattices · Silica

## Introduction

Graphene (G) and graphene oxide (GO) have several advantages as adsorbents, but their practical use in classical SPE can be hampered because their reduced particle sizes. GO has an additional advantage: it can be easily doped. Since doped-carbon materials with different elements such as boron, nitrogen, or other elements have attracted the interest of numerous scientists due to its unique electronic properties that result in exceptional performance for applications in electronics or catalysis [1, 2]. Important of GO is attributed to the low cost of its production, its accessibility, and the possibility of transferring it to graphene on a large scale. RGO attracted the physicists due to its electronic behavior

under magnetic field and at low temperature. RGO's transform properties from microscopic to molecular scales have attracted considerable attention to current research effort [3]. The recently emerging graphene-based materials, e.g., GO nanosheets have drawn world attention owing to their superior hydrophilic properties resulted from bulk amount of oxygen functionalities such as hydroxyl, epoxy, and carboxyl [4]. Fortunately, there are many synthetic strategies to produce RGO quality in huge amounts of GO at actual cost [5].

Nevertheless, the isolated graphene oxide monolayer has gained double attention and within a few years the researchers will be able to check the characteristics of this fresh yet ancient two-dimensional material [6]. At present, the technique used by Hummers to generate RGO has been commonly embraced, but it still suffers from several flaws such as poisonous gas generation (NO<sub>2</sub>, N<sub>2</sub>O<sub>4</sub>), residual nitrate and low yield, etc. Graphene oxides show important variations in their features based on the synthesis technique and the degree of oxidation [1, 7–9]. Also, a large difference is noted in the hydration and solvation properties of GOs prepared by Brodie and Hummers, respectively [1]. Recently, using of a mixture of H<sub>2</sub>SO<sub>4</sub> and KMnO<sub>4</sub> to cut long-standing carbon nanotubes lead to produce a microscopic flat strips of GOs and a few wide carbon atoms that have edges “capped” by oxygen atoms (=O) or hydroxyl groups (–OH) [1].

✉ Mahmoud Fathy  
fathy8753@yahoo.com

<sup>1</sup> Applications Department, Egyptian Petroleum Research Institute (EPRI), 1 Ahmed El-Zomer, Nasr City, Box. No. 11727, Cairo, Egypt

<sup>2</sup> Faculty of Science, Benha University, Fred Nada Street, Banha, Egypt

<sup>3</sup> Engineering Sciences Department, of Engineering, Beni-Suef University, Beni-Suef, Egypt

<sup>4</sup> Department of Chemistry, Faculty of Science, (Girls), Al-Azhar University (Girls), Nasr City, Cairo, Egypt

Bottom-up or (Tang-Lau technique) is another technique for the preparation of graphene oxide, the sole source of which is glucose, and distinguished by its safer, easier, layer width control, varying from monolayer to multilayer by regulating growth factors, and lastly its more environmentally friendly compared to the conventional “top-down” technique. [10–13]. Because the precise composition of RGO is difficult to describe, the past study stated that RGO is a communicable graphene aromatic lattice that impedes epoxides, alcohols, ketones, and *n* carboxylic groups. Such obstruction of the lattice is indicated by increasing the spacing of the interlayer to 0.335 nm and 0.625 nm respectively for graphene and RGO. On the other side, flake graphene is naturally.

Water is the most essential element to sustain all living organisms. Unfortunately, it is being subjected to harmful contamination by various industrial operations, the use of different vehicles and by the waste of many industries based upon new technologies which have been developed in order to fulfill the demands of this modern era and generate wastes more than ever. Each source of contamination has its own destructive effects on plants, animals, and ultimately on human health, but contamination of heavy metals in water is of serious concern due to their persistence in the environment and carcinogenicity to human beings. The bromophenol blue dye contaminate waters by many industries such as mining, tanneries, metal smelting, and batteries. As these metals cannot be degraded biologically, their contamination in water becomes a potential threat for the entire ecosystem starting from microorganisms to human beings. In addition organic dyes released from paper, plastic and cosmetic industries are also other source of contaminants for waters that are discharged from industrial wastes. The presence of these dyes in environment, specifically in water, can cause some severe effects on living organism and human health such as cyanosis, jaundice, shock, vomiting, quadriplegia, tissue necrosis, and increase in heartbeat. Some dyes and their degradation products are so toxic that they are considered as carcinogenic.

Nevertheless, most of published methods using nanomaterials as sorbents are dedicated to the adsorption/determination of positive ions like Cr(III), Fe(III), Co(II), Ni(II), Cu(II), Zn(II), Cd(II), and Pb(II) [8–10] and organic compounds [3, 11]. Sorption and determination of anionic forms of elements is much more difficult, but it is also necessary and important. The ultrahigh specific surface area of graphene is responsible for its high chemical activity as well as high adsorption capacity. However, metal ions can be often adsorbed on graphene nanosheets only as hydrophobic complexes using chelating agents. Therefore, the development of functionalized graphene is recommended particularly in the context of the anionic species adsorption as well as the enhancement of its selectivity.

In the present study, GO is processed from microcrystalline cellulose using catalytic acid spray (CAS) method, without attaining zero temperature and the addition of toxic chemicals

( $\text{NaNO}_2/\text{NaNO}_3$ ). The final samples were characterized by XRD, Raman, FTIR, TEM, and UV-spectroscopic techniques, and the results are discussed. The effects of pH and adsorbent dosage on bromophenol blue dye adsorption from aqueous solution were studied through batch technique. Adsorption kinetics, equilibrium isotherms, and thermodynamic studies were conducted to study the adsorption mechanism of bromophenol blue dye on RGO. This study highlights the extensive applicability of this novel material in the management of bromophenol blue dye containing wastewater.

## Material and methods

### Materials

Sulfuric acid ( $\text{H}_2\text{SO}_4$ ) 98%, cobalt nitrate ( $\text{Co}(\text{NO}_3)_2$ ), cetyltrimethylammonium bromide (CTAB), sodium hydroxide (NaOH), TEOS, bromophenol blue dye, and silica were used as they are without purifying.

### Catalytic acid spray method for preparing RGO

#### Preparation of silica cobalt nanocomposite catalysis

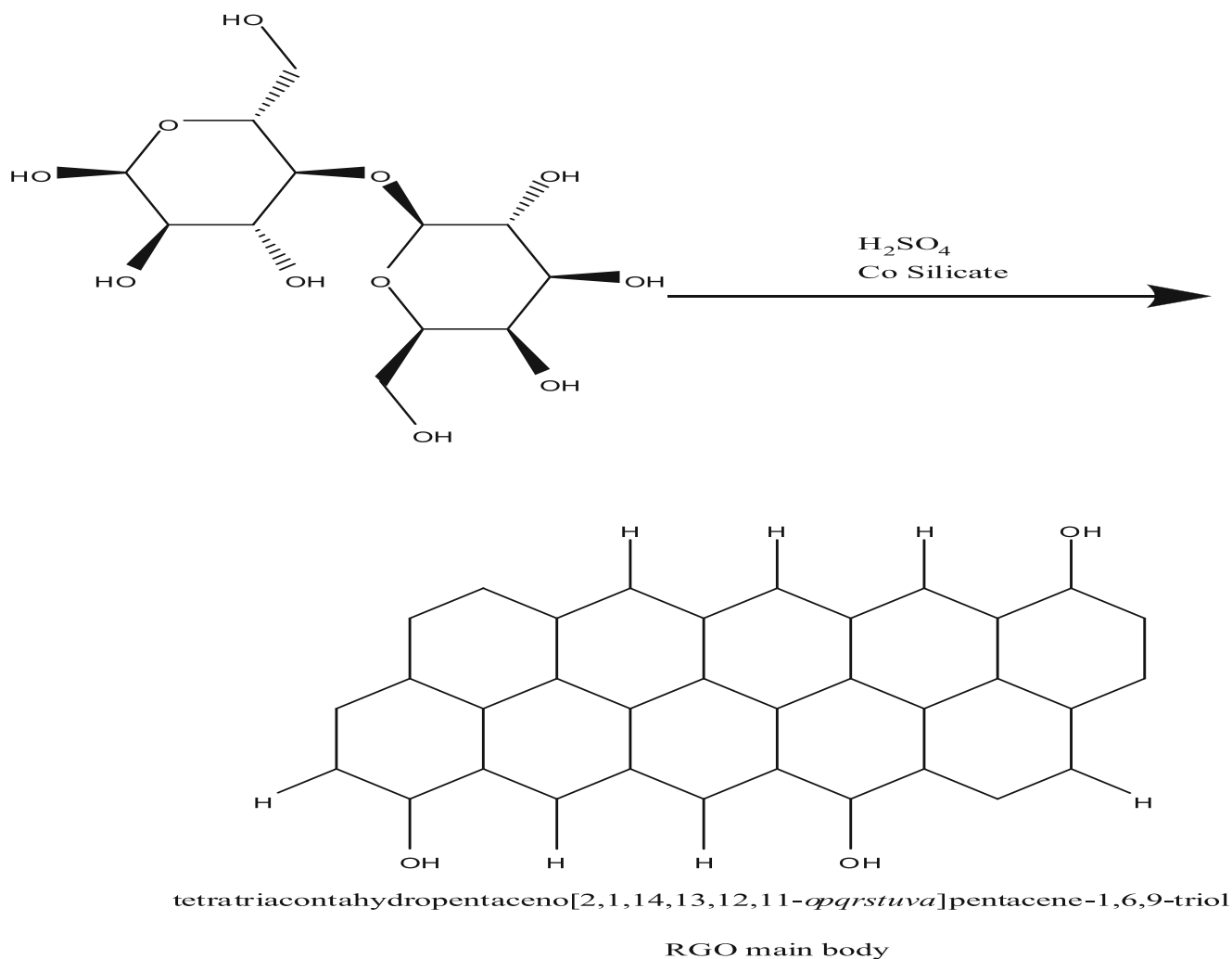
Direct precipitation method was typically used by 16.2 g of cetyltrimethylammonium bromide (CTAB) dissolved in a solution containing 145 ml of deionized water at 30 °C [14]. After that, 8.21 ml of tetra ethyl orthosilicate (TEOS) as a silicon source and 32 ml of 30 percent  $\text{NH}_3$  were then added drop wise and stirred vigorously for 12 h to hydrolyze TEOS with 0.5 g cobalt nitrate. The product obtained was filtered and overnight dehydrated under vacuum at 40 °C. The samples were annealed at 550 °C in atmosphere for 4h to remove surfactant, after which the MCM-41 (Mobil Composition of Matter No. 41) was achieved [15].

#### Extraction of amorphous microcrystalline cellulose

Hemicellulose fraction in wood waste was hydrolyzed for 60 minutes at 120 °C with 1% (wt/wt)  $\text{H}_2\text{SO}_4$  to enter the hydrolysate portion as monomeric sugars. The resulting residue (microcrystalline cellulose) was then subjected to the delignification method using a combination of 1.5% (wt/wt) NaOH and 0.5% (wt/wt)  $\text{H}_2\text{O}_2$  at 120 °C for 60 min. Lignin and silica present in the pretreated timber waste were transferred to the black liquor during the alkaline peroxide delignification process [3].

#### Preparation of RGO nanosheets

One gram of silica was put in 100-mL round-bottom flask, and 5 g microcrystalline cellulose was then added and dosed by



**Scheme 1** The exfoliation of RGO from microcrystalline cellulose by CAS method

5 mL concentrated  $\text{H}_2\text{SO}_4$ , then left for 10 min; after that, it was filtrated, washed with boiling water till pH 7, and kept in oven at 40 °C for 6 h as shown in the preparation and mechanism of reaction in Scheme 1. The prepared carbon material was decanted in a flask with 0.01 g cobalt silicate nanoparticles and heated to 40 °C for 40 min to obtain agglomerated GO sheet. Then, the agglomerated GO sheet was left to cool for 2 h, and then treated with 30 mL biphenyl anime to produce RGO sheets that was dehydrated at 50–80 °C for 48 h to obtain exfoliated single-layer RGO [16].

### Characterization and evaluation

The morphologies of RGO were observed using a transmission electron microscope (Hitachi S-4800). The construction of the RGO was analyzed with an image analyzer (Image Pro Plus 5.0). The diameters of the RGO were calculated by averaging 100 measurements using the same analysis software. The FTIR spectra were measured using a Nicolet 5700

spectrometer (Nicolet) by tableting with KBr. The changes to the crystalline form were determined by XRD using the X'Pert Pro MPD X-ray diffraction system (PAN analytical, The Netherlands). The samples were measured at 40 kV of the acceleration voltage and 40 mA of supplying current by Cu K $\alpha$  radiation (k50.154 nm). The XRD profiles were recorded with the diffraction angle (2  $\theta$ ) ranging from 58 to 458 at a scanning speed of 58  $\text{min}^{-1}$ . The pyrolytic behaviors of the RGO in  $\text{N}_2$  was characterized by a thermogravimetric-differential thermal analysis (TG-DTA, TG8120, Rigaku, Japan). The Raman spectra were measured using a Micro-Raman Spectrometer (LabRAM XploRA, HORIBA Scientific, France). A light source with 532-nm radiation from a semiconductor laser was used.

### Adsorption experiments

The effect of pH was investigated by adjusting the solution pH from 2 to 10. The effect of adsorbent dosage on bromophenol

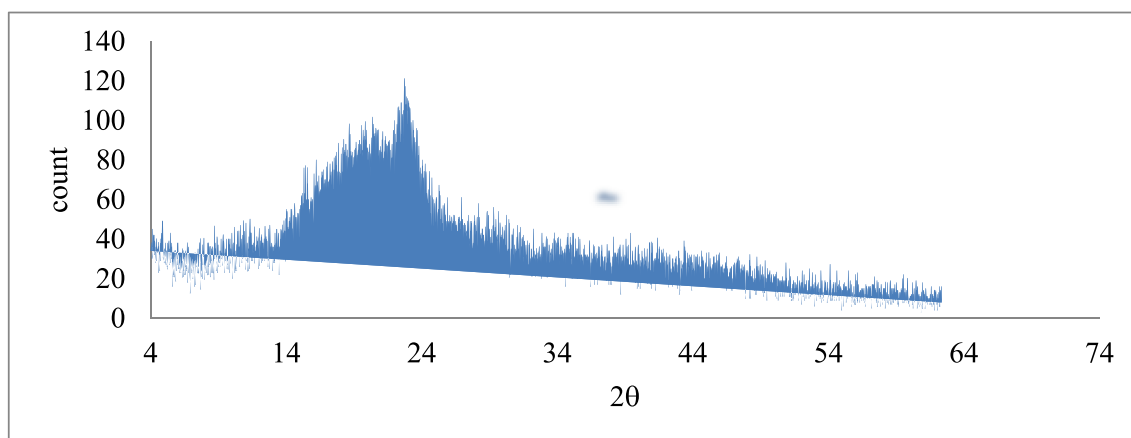


Fig. 1 XRD of reduced graphene oxide

blue dye adsorption was studied by changing the mass of RGO from 0.01 to 0.5 g. In sorption kinetics studies, 0.01 g of RGO was added into 25 mL of  $15 \text{ mg L}^{-1}$  bromophenol blue dye aqueous solution under pH 7 at 303 K, and the solution was sampled at a given reaction time interval. For equilibrium isotherm studies, 0.01 g of RGO was dispersed and stirred in 25 mL of bromophenol blue dye solutions with initial concentrations ranging from 5 to  $100 \text{ mg L}^{-1}$  under

neutral pH. The solutions were stirred until adsorption equilibrium was reached.

All bromophenol blue dye adsorption experiments were performed in batch solution in an air bath shaker ( $160 \text{ r min}^{-1}$ ). The aqueous solution was separated from RGO particles through membrane filtration, and the concentrations of the remaining bromophenol blue dye were measured with a T6 UV–Vis spectrophotometer.

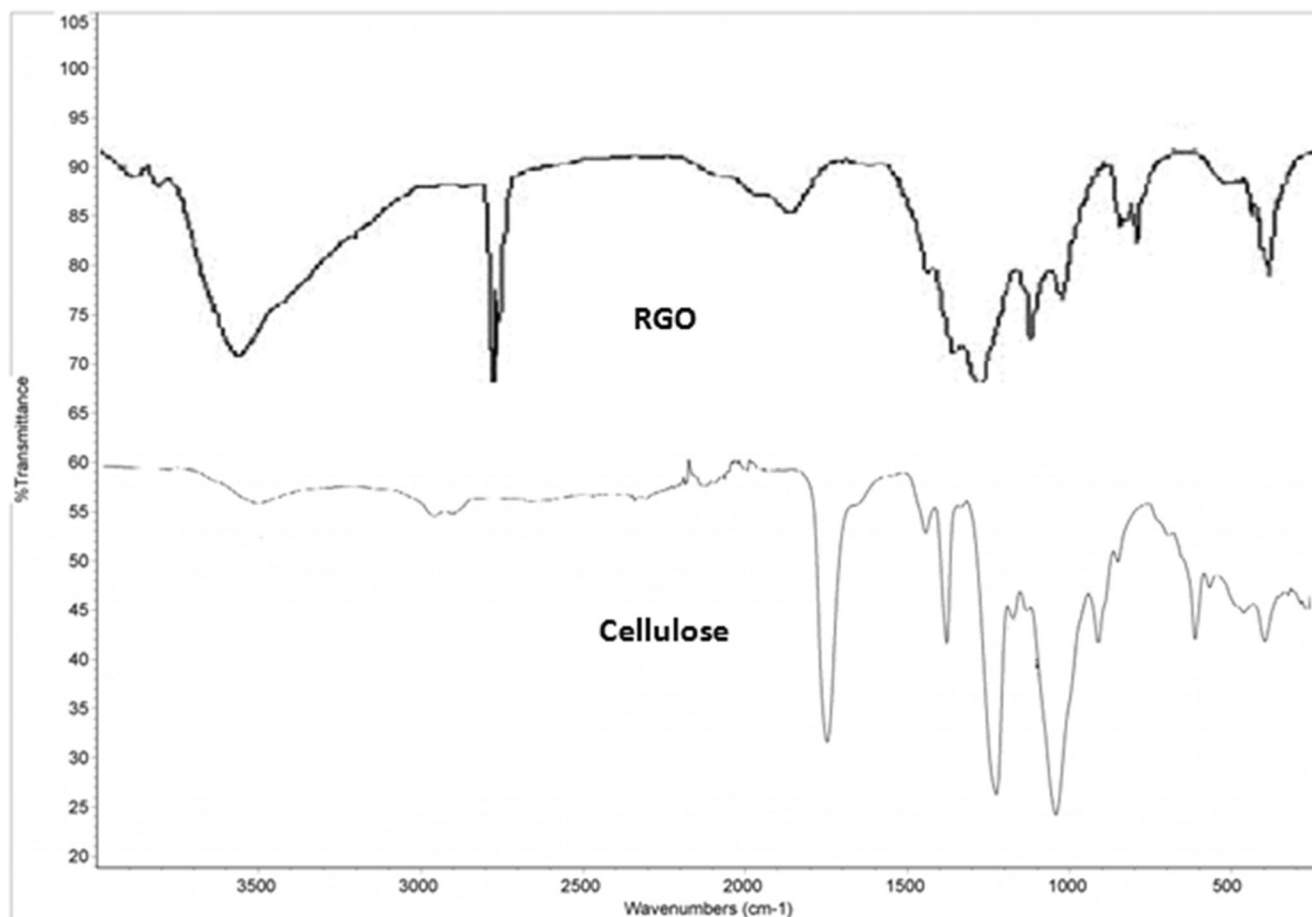


Fig. 2 FTIR of cellulose and prepared graphene oxide by CAS method

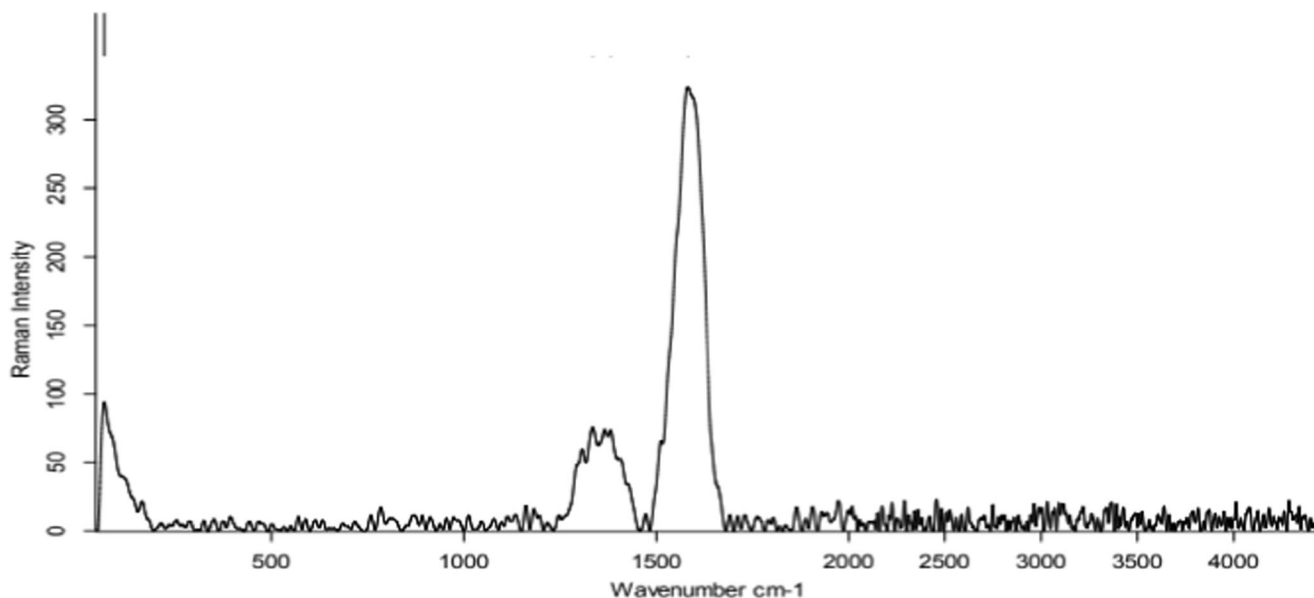


Fig. 3 Raman spectroscopy of graphene oxide that produced from cellulose

## Results

### Analysis using XRD

As shown from the XRD pattern of RGO (Fig. 1), the presence of inset distance between the layers has a significant consideration for described the structural aspects of graphene. However, the (001) peak has been shifted to  $13.05^\circ$  for RGO with a d-spacing value of 2.7997 nm. Increasing of spacing between layers is indicating on the inserted of water moieties with oxygen functionalities of RGO [17, 18]. From the XRD patterns, parent graphite shows a very sharp peak at

$2\theta = 26.5^\circ$  which corresponds to (002) plane with an interlayer distance of 0.342 nm in addition to small peaks at  $2\theta = 44.56^\circ$  and  $77.51^\circ$  are associated with original graphite powder.

As we seen from XRD pattern of Co/silica catalysts, three intensive peaks are observed at  $21^\circ$ ,  $29^\circ$ , and  $60^\circ$ , corresponding to 002, 100, 101, and 004 reactions, respectively. RGO shows maximum broad band and sharp peak measured at  $22.25^\circ$  and  $24.27^\circ$ , respectively [19].

We can suggested that the broad band appeared in XRD pattern of RGO may due to combine of graphene sheets with another layers produced as a result of different intercalation and de-intercalation stages of silicate content of catalyst or the cellulosic

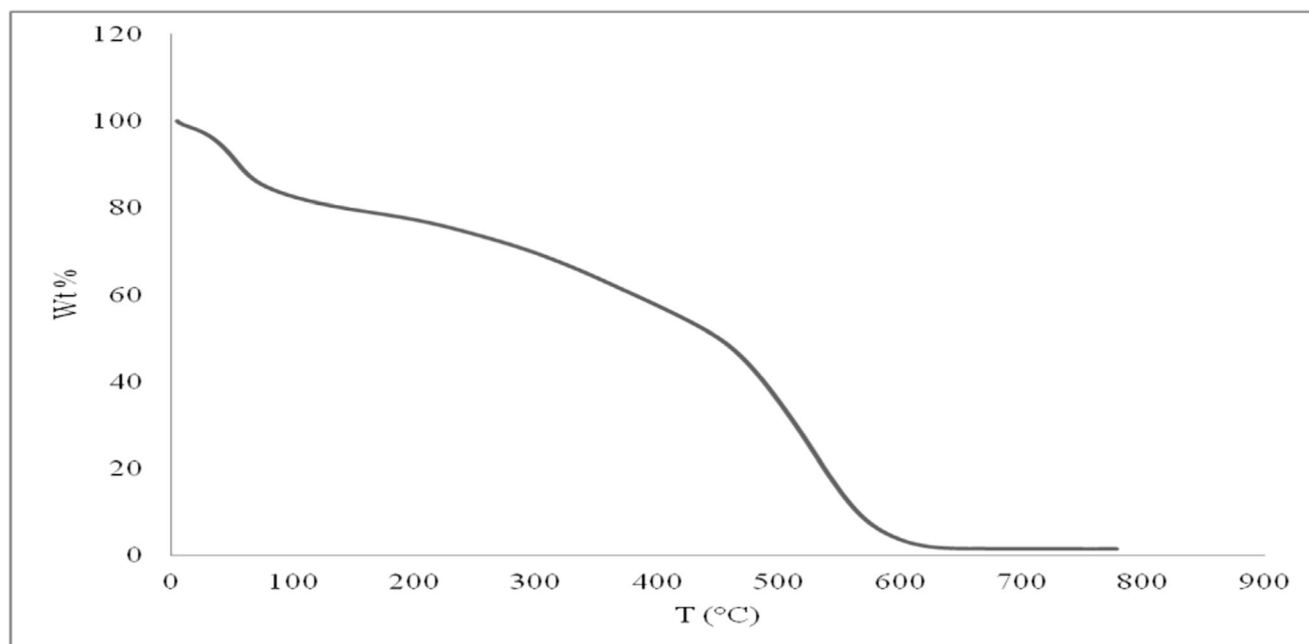
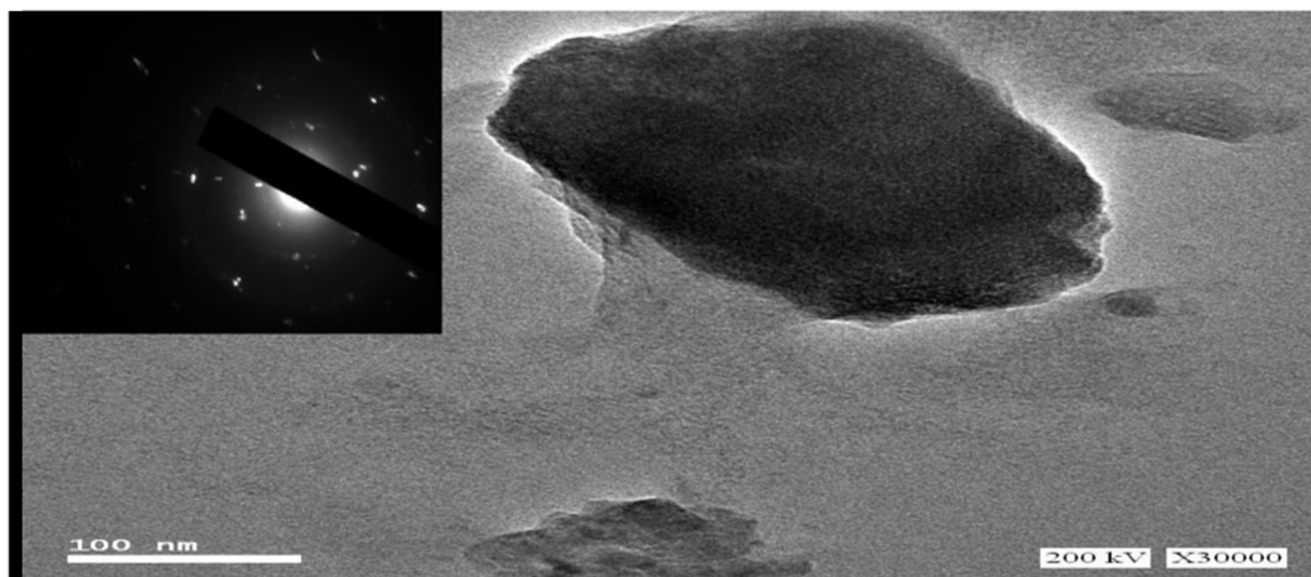


Fig. 4 TGA of RGO nanoparticles



**Fig. 5** HRTEM and SAED of reduced graphene oxide sheets

precursor materials. Also, we found that the d-spacing values ranging between 1.23 and 0.85 nm calculated using Bragg equation [20].

### Infrared spectra

FTIR of cellulose in Fig. 2 showed an absorbance at  $3550\text{ cm}^{-1}$  band that attributed to stretching of the O–H bond (hydroxyl groups) of cellulose. Furthermore, an increase is observed for the bands around  $2920\text{ cm}^{-1}$  assigned to the C–H stretching, due to the presence of the CH– and CH<sub>2</sub>– groups of the cellulose and CH<sub>3</sub>– of the cellulose. The  $1638$ ,  $1417$ ,  $1300$ ,  $1161$ ,  $1046$ , and  $895\text{ cm}^{-1}$  bands were attributed to C–H stretching of CH<sub>2</sub> and CH<sub>3</sub> groups. In Fig. 2, we can see a strong peak at  $1570\text{ cm}^{-1}$  was observed, owing to the C=O stretching of COOH group of RGO [21]. FTIR spectrum in Fig. 2 shows the presence of bulk amounts of oxygen functional groups in RGO such as OH stretching, stretching vibration in COOH, unoxidized *sp*<sup>2</sup> aromatic C–C bonds, –OH deformation, and C–O stretching vibration in alkoxy and epoxy groups. The

detection of strong signal at  $3393\text{ cm}^{-1}$  is the main factor causing RGO to be superhydrophilic in nature [22].

The FTIR of RGO (Fig. 2) exhibits three characteristic peaks at  $1300$ ,  $1710$ , and  $3450\text{ cm}^{-1}$  for carboxylic acids, carbonyl groups, and hydroxyl groups, respectively [23]. The bands at  $1249$  and  $1134\text{ cm}^{-1}$  can ascribed by asymmetric and symmetric S=O, respectively. This means that we successfully prepared RGO having functional surface modification [24]. There was a strong decrease in the intensities of the characteristic absorption bands of oxygen functional groups (carboxy, epoxy, alkoxy, and hydroxyl) and was removed effectively by acetone treatment at low temperature. This further indicates that GO had been reduced to graphene sheets, which is consistent with the XRD results.

### Raman spectroscopy

Raman spectroscopy was used to detect the quality of prepared graphene sheets, and that is a powerful candidate for quick and nondestructive inspection of many layers of

**Fig. 6** Effect of solution pH on the bromophenol blue dye sorption on RGO,  $20\text{ mg L}^{-1}$  bromophenol blue dye in  $100\text{ mL}$  solution, temperature  $298\text{ K}$ , adsorbent dosage  $0.1\text{ g}$

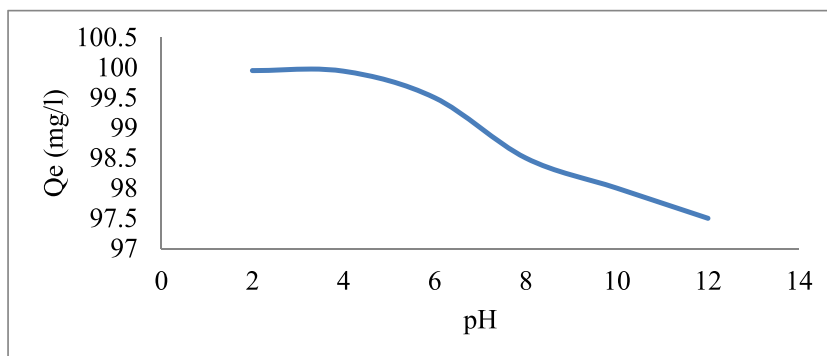
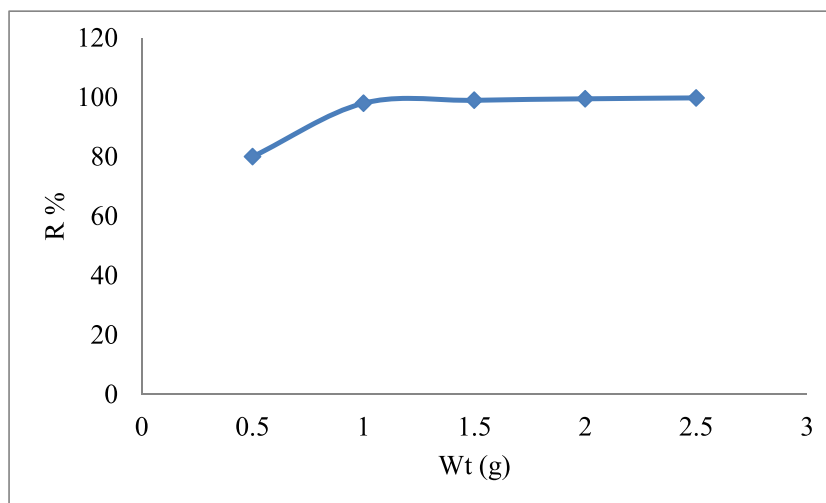


**Fig. 7** Effect of ionic strength on the bromophenol blue dye adsorption on RGO under different adsorbent dosage



graphene [25, 26]. Raman spectroscopy of RGO was used to verify the presence of graphene.

The spectrum of RGO in Fig. 3 shows the intense peaks at  $1348\text{ cm}^{-1}$  (D) and  $1558\text{ cm}^{-1}$  (G). The G bands that exist in all *sp*<sup>2</sup>-hybridized carbon materials is due to stretching of the C–C bond; meanwhile, the D and D' bands resulted from the disorder in the graphene flakes. The 2D band is slightly broader, between  $2650$  and  $2700\text{ cm}^{-1}$  and very small that indicate very far sheets of RGO. The outcome results recommend that the prepared graphene sheets of graphene could be single sheet. Previous studies recommended that the graphene obtained by the reducing chemical method displays two distinguishing main peaks: G band at  $1575\text{ cm}^{-1}$  and the D band at  $1350\text{ cm}^{-1}$ . Here, we detected that RGO display G band at  $1558\text{ cm}^{-1}$  and D band at  $1348\text{ cm}^{-1}$  separately (Fig. 5). The G band of RGO showed a red-shift from  $1557$  to  $1558\text{ cm}^{-1}$ , and is known as regaining of carbon atoms in a hexagonal system. The intensity ratio IG/ID is used to assess the amount of defects in graphene and the in-plane crystallite. Here, the ID/IG values are estimated to be around 3 for sample RGO. A higher ratio value can be translated to the decrease in *sp*<sup>2</sup> domain due to the reduced size of GO sheets after reduction. This is also due to the defects created after the removal of oxygen functionalities like epoxides, the predominant formation of ketone and carboxylic acid functionalities on the edges of GO sheets, and the restoration of the graphitic *sp*<sup>2</sup> network [27] [24, 28].

### Thermal analysis

TGA curve of GO in Fig. 4 indicates the thermal stability of the nanosheets. The minimum weight loss before  $100\text{ }^{\circ}\text{C}$  is due to the release of trapped water between RGO nanosheets while significant weight loss between  $282$  and  $640\text{ }^{\circ}\text{C}$  is attributed to the decomposition of less-stable oxygen functional groups in RGO. Other more stable functional groups only start to decompose after  $230\text{ }^{\circ}\text{C}$ . [29].

The higher degradation residues of RGO proposed that some impurities from silica and the catalyst are involved in synthesis process and may contributed to produce yield over 100% of some samples [30]. Overall, the RGO displayed good thermal stability, and no major weight loss was found. The above results confirm that the RGO have been successfully fabricated.

### The structure analysis of RGO

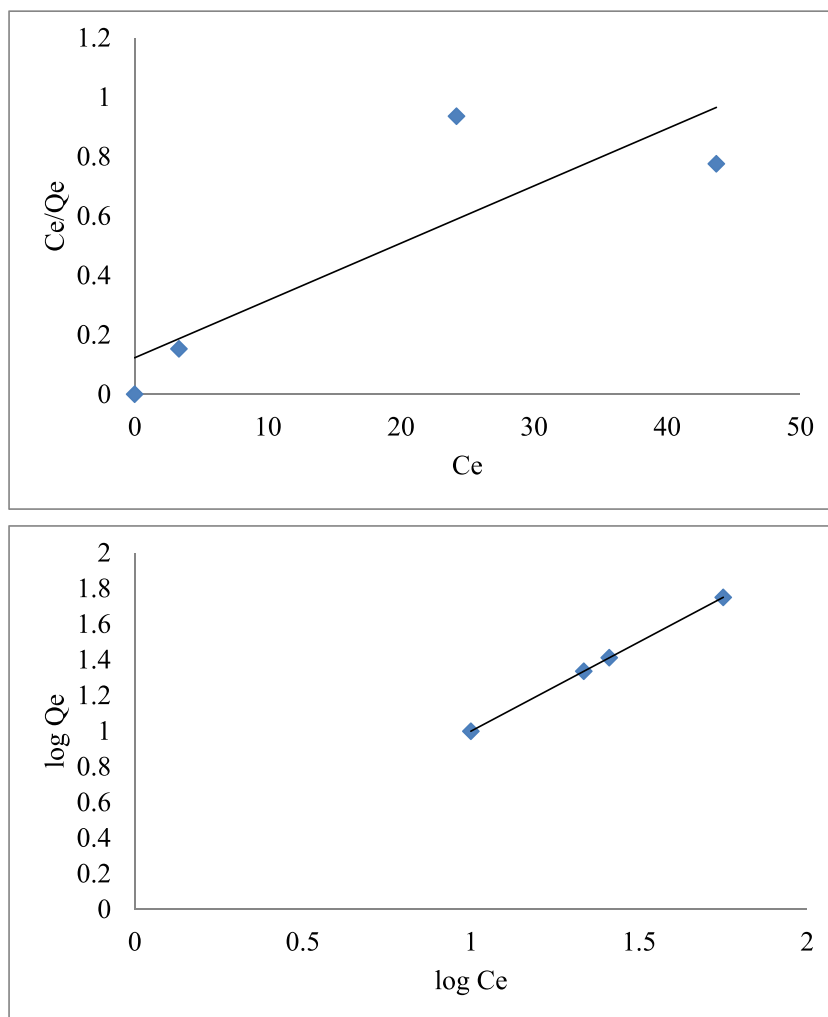
HR-TEM images of the GO nanoparticle sheets in Fig. 5 show that the distance between GO layers was about 1 nm which is more than the interlayer distance of graphite, suggesting the growth of the few-layer of GO on the surface of the Co-silicate nanoparticles.

Also, as seen in Fig. 5, GO flakes are separated from each other and indicates the formation of single order of the RGO sheets; also, the well-ordered hexagonal graphite lattices of monolayered RGO flakes are obviously indicated on the succeeding preparation of RGO by CVD method [1]. The appearance of spherical beadlike Co-silicate particles on the smooth layer of graphene can be seen in Fig. 8, which is attributed to increase in the surface area. Also, we can see that the surfaces of the RGO with a uniform diameter were

**Table 1** Kinetic parameters of pseudo-first-order and pseudo-second order models for the bromophenol blue dye removal using RGO

Pseudo-first-order kinetic model			
$k_1$ ( $\text{min}^{-1}$ )	$q_e$ ( $\text{mg g}^{-1}$ )	$R^2$	AARE (%)
0.050	1–32	0.4066	7
Pseudo-second-order kinetic model			
$k_2$ ( $\text{g mg}^{-1} \text{min}^{-1}$ )	$q_e$ ( $\text{mg g}^{-1}$ )	$R^2$	AARE (%)
0.0374	54.2	1	2.93

**Fig. 8** Langmuir (a) and Freundlich isotherms (b) of bromophenol blue dye adsorption on RGO



smooth, but some beads were found on the surface of RGO, which were mainly attributed to the agglomeration of catalyst and the interference among the RGO.

As evident (Fig. 6) of SAED, the spots like, corrugated morphology of RGO was well preserved despite the high and homogeneous coverage of Co-silicate nanoparticles. The vast majority of the Co-silicate nanoparticles were found well dispersed on the RGO skeleton, and it should be emphasized that, without the presence of the RGO, Co-silicate nanoparticles tend to aggregate into large clusters

due to the coalescence. [26]. Taking into consideration that the typical precision of HRTEM analysis is generally not exceeded than a few percent, thereby, the notable lattice margins can be attributed to the catalyst and the flat surface of RGO, respectively [31].

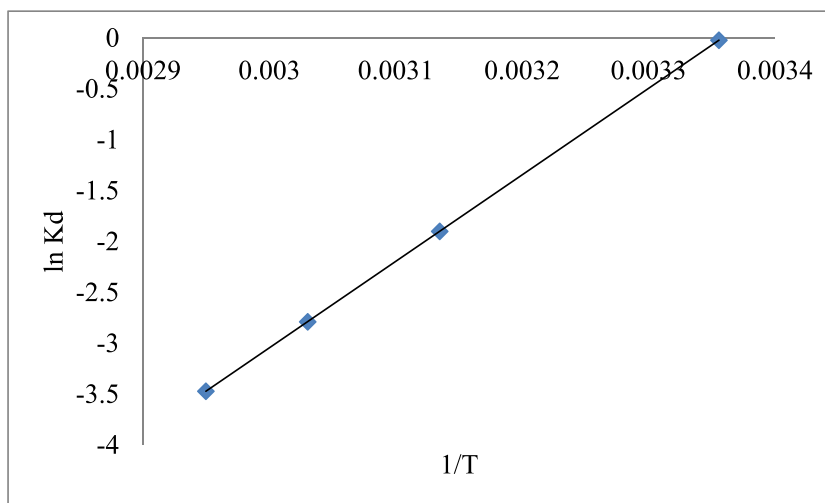
### Effect of pH

The effects of pH on bromophenol blue dye adsorption onto RGO was investigated through batch technique over a pH

**Table 2** Langmuir and Freundlich isotherm parameters of bromophenol blue adsorption on RGO and their correlation coefficients.

Models	$T$	Isothermal parameters
Freundlich	298	$R^2 = 0.992$ , $n = 1.6992$ , $K_F = 16.6695$
	319	$R^2 = 0.9893$ , $n = 1.2285$ , $K_F = 23.2381$
	330	$R^2 = 0.9954$ , $n = 1.2329$ , $K_F = 24.711$
Langmuir	298	$R^2 = 0.9320$ , $q_{\max} = 17.94 \text{ mg g}^{-1}$ , $K_L = 0.0725 \text{ L mg}^{-1}$
	319	$R^2 = 0.9243$ , $q_{\max} = 24.19 \text{ mg g}^{-1}$ , $K_L = 0.0930 \text{ L mg}^{-1}$
	330	$R^2 = 0.9321$ , $q_{\max} = 37.78 \text{ mg g}^{-1}$ , $K_L = 0.0342 \text{ L mg}^{-1}$

**Fig. 9** Plots of  $\ln K_D$  vs.  $1/T$  for the bromophenol blue removal on RGO



range of 2–10. As illustrated in Fig. 6, bromophenol blue dye adsorption on RGO drastically increased as pH increased from 2 to 7 but decreased as pH further increased from 8 to 10. This trend can be mainly attributed to the effects of solution pH on bromophenol blue dye and adsorbent surface properties. At low pH, the high concentration of H<sup>+</sup> competes with bromophenol blue dye for adsorption on the active sites of the adsorbents, thus reducing bromophenol blue dye adsorption [30]. At high pH, the surfaces of the adsorbents become negatively charged due to deprotonation, and hydrolyzed bromophenol blue dye by-products are produced [32]. Thus, the enhancement of electrostatic attraction between the positive charges of cations and the negative charges of adsorbents improves the adsorption capacity of bromophenol blue dye. In the pH range from 8 to 10, the hydrolysis of bromophenol blue dye further strengthened given that high pH caused the formation of bromophenol blue dye precipitants, and electrostatic repulsion between the negative charges of cations and the negative charges of adsorbents would then inhibit the sorption of bromophenol blue dye. Similar phenomena have also been observed elsewhere [22].

### Effects of RGO dosage

The effect of solid dosage on bromophenol blue dye sorption on RGO is shown in Fig. 7. Bromophenol blue dye adsorption percentage increased with increasing RGO dosage but did not change when composite dosage exceeded 1.5 g. Sorption efficiency (*R*%) decreased rapidly from 80 to 100% with increasing adsorbent dosage. This behavior can be attributed to the increased availability of active sorption sites with the increase in RGO dosage. Additional active sorption sites increase sorption percentage by increasing the sorption binding points of bromophenol blue dye to RGO. However, the load on the unit surface area decreased to decrease sorption quantity.

### Analysis of adsorption kinetics

In order to examine the controlling mechanism of the adsorption process, kinetic models were used to test the experimental data. The pseudo-first-order equation is one of the most widely used rate equations to describe the adsorption of an adsorbate from the liquid phase. The pseudo-first-order equation is generally expressed as follows:

$q_t = q_e(1 - e^{-k_1 t})$  where  $q_e$  and  $q_t$  (mg g<sup>-1</sup>) are the amounts of ammonium ions adsorbed at equilibrium and at time  $t$  (min), respectively, and  $k_1$  is the pseudo-first-order rate constant (min<sup>-1</sup>).

The pseudo-second-order model is more suitable for the description of the kinetic behavior of adsorption in which chemical sorption is the rate-controlling step. The pseudo-second-order equation is given by [36, 37]:

$t/q_t = 1/k_2 q_e^2 + (1/q_e)t$  where  $k_2$  (g mg<sup>-1</sup> min<sup>-1</sup>) is the rate constant of the pseudo-second-order equation.

Table 1 presents the data for bromophenol blue dye adsorption on RGO at different time intervals. Bromophenol blue dye was rapidly taken up by RGO, and adsorption equilibrium was reached almost instantaneously (10 min). The adsorption kinetics of RGO was analyzed to further illustrate bromophenol blue dye sorption behavior. Table 1 show that the pseudo-first-order model of bromophenol blue dye onto RGO exhibited poor correlation with experimental sorption data, and Table 1 shows that sorption capacity at various intervals was fitted by the pseudo-second-order model.

**Table 3** Thermodynamic parameters for the bromophenol blue removal on RGO

<i>T</i>	$\Delta S^\circ$	$\Delta H^\circ$	$\Delta G^\circ$
298	165.7863	47,722.97	- 581.89
319			- 7821.23
330			- 6806.76

## Adsorption isotherm

The equilibrium adsorption isotherms of bromophenol blue dye on RGO at 293, 303, and 313 K are shown in Fig. 8. It indicated the adsorbed amount of adsorption isotherm was the lowest at  $T=293$  K and the highest at  $T=313$  K. Adsorption isotherms are used to improve the understanding of the adsorption mechanisms between the adsorbent and adsorbate [60]. To confirm the mechanistic parameters of bromophenol blue dye adsorption, experimental data were analyzed on the basis of the well-known Langmuir and Freundlich isotherm models. The linear forms of the Langmuir isotherm and Freundlich isotherm models are expressed as:

$$q_e = \frac{q_m K_L C_e}{1 + K_L C_e}$$

where  $q_e$  ( $\text{mg g}^{-1}$ ) is the equilibrium bromophenol blue dye concentration on the sorbent,  $C_e$  ( $\text{mg L}^{-1}$ ) is the equilibrium bromophenol blue dye concentration in the solution,  $q_m$  ( $\text{mg g}^{-1}$ ) is the maximum monolayer adsorption capacity ( $\text{mg g}^{-1}$ ), and  $K_L$  is the Langmuir sorption constant ( $\text{L mg}^{-1}$ ) relating the free energy of sorption; a high value indicates a higher affinity.

The Freundlich isotherm model proposes a monolayer adsorption with a heterogeneous energetic distribution of active sites, accompanied by interactions between adsorbed molecules. The Freundlich model can be expressed as [30]:

$$q_e = K_F C_e^{1/n}$$

where  $K_F$  is a constant relating the adsorption capacity and  $1/n$  is an empirical parameter relating the adsorption intensity, which varies with the heterogeneity of the material.

The experimental results showed that data for the adsorption of bromophenol blue dye onto bromophenol blue dye under 293, 303, and 313 K are better fitted with Freundlich isotherms (Fig. 8) than with Langmuir isotherms. These results suggested that bromophenol blue dye sorption on RGO is heterogeneous. Langmuir and Freundlich isotherm parameters and their correlation coefficients for RGO are listed in Table 2. An increase in  $K_F$  with an increase in temperature indicated that the sorption capacity of bromophenol blue dye onto RGO increased with increasing temperature; thus, bromophenol blue dye sorption on bromophenol blue dye can be endothermic [12, 49]. The maximum sorption capacity of RGO was  $234.19 \text{ mg g}^{-1}$  at 303 K, which is comparable with those of previously reported RGO for bromophenol blue dye.

## Thermodynamic studies

The  $\Delta H^\circ$ ,  $\Delta S^\circ$ , and  $\Delta G^\circ$  data of the adsorption process were obtained by using the following equations [2, 65]:

$$\ln K_D = \frac{\Delta S^\circ}{R} - \frac{\Delta H^\circ}{RT}$$

where  $K_D$  is the distribution coefficient ( $\text{mL g}^{-1}$ ),  $\Delta H^\circ$  is the enthalpy change ( $\text{kJ mol}^{-1}$ ),  $\Delta S^\circ$  is the entropy change ( $\text{J mol}^{-1} \text{K}^{-1}$ ),  $T$  is the temperature (K), and  $R$  is the universal gas constant ( $8.314 \text{ J mol}^{-1} \text{K}^{-1}$ ). The Gibbs free energy change ( $\Delta G^\circ$ ) is calculated from the following equation:

$$\Delta G^\circ = \Delta H^\circ - T\Delta S^\circ$$

Based on this equation, the  $\Delta H^\circ$  and  $\Delta S^\circ$  parameters can be calculated from the slope and intercept of the plot of  $\ln K_D$  versus  $1/T$ , respectively (Fig. 9).

Table 3 shows the values of the thermodynamic parameters of bromophenol blue adsorption on RGO. Negative  $\Delta G^\circ$  values indicate that a sorption process is spontaneous [65]. Positive  $\Delta H^\circ$  values obtained in this study indicated that bromophenol blue sorption on RGO is an endothermic process, and the positive  $\Delta S^\circ$  values implied an increase in randomness at the RGO solution interface during the bromophenol blue sorption process.

## Conclusion

The present work was focused on developing a good strategy for preparing RGO. XRD, Raman, HR-TEM, and XRD evaluations confirmed the formation of the RGO. Our current findings offer an environmentally friendly and a profitable method for producing stable RGO; this method can be adjusted for bulk production. According to our experience, this is the first example for CAS method to produce RGO. It has been found that the adsorption of RGO is strongly affected by the dosage and initial pH of the solution. The adsorption process follows the pseudo-second-order kinetic model. The experimental data were well fitted to the Freundlich equation, with good correlation coefficients. The negative values of  $\Delta G^\circ$  indicate the spontaneous nature of the adsorption process. The adsorption process was found to be endothermic as confirmed by the positive sign of the enthalpy ( $\Delta H^\circ$ ). The entropy change ( $\Delta S^\circ$ ) is positive indicating increasing randomness at the solid–solution interface during adsorption. So, these RGOs can be used as adsorbents for the quick removal of a variety of contaminations from various waters while their nanosize and magnetic behavior offers their easy removal from the water upon the completion of adsorption task.

## References

1. Fathy, M., et al.: Incorporation of multi-walled carbon nanotubes in microspheres used as anion exchange resin via suspension polymerization. *Appl. Nanosci.* **4**(5), 543–549 (2014)

2. Ramzi, M., Hosny, R., El-Sayed, M., Fathy, M., Moghny, T.A.: Evaluation of scale inhibitors performance under simulated flowing field conditions using dynamic tube blocking test. *Int. J. Chem. Sci.* **14**(1), 16–28 (2016)
3. Farrag, A.E.H.A., Moghny, T.A., Gad, A.M., Saleem, S.S., Fathy, M., Ahmed, M.A.: Removing of hardness salts from groundwater by thermogenic synthesis zeolite. *SDRP J. Earth Sci. Environ. Stud.* **4**(2), 109–119 (2016)
4. Farrag, A.E.H.A., Moghny, T.A., Gad, A.M., Saleem, S.S., Fathy, M.: Abu Zenima synthetic zeolite for removing iron and manganese from Assiut governorate groundwater, Egypt. *Appl. Water Sci.* **7**(6), 3087–3094 (2016). <https://doi.org/10.1007/s13201-016-0435-y>
5. Farrag, A., et al.: Removing of hardness salts from groundwater by thermogenic synthesis zeolite. *J. Hydrogeol. Hydrol. Eng.* **5**, 4 (2016). [https://doi.org/10.4172/2325\\_9647](https://doi.org/10.4172/2325_9647)
6. Fathy, M., Moghny, T.A., Allah, E.A., Alblehy, A.E.: Cation exchange resin nanocomposites based on multi-walled carbon nanotubes. *Appl. Nanosci.* **4**(1), 103–112 (2014)
7. Fathy, M., et al.: Nano composites of polystyrene divinylbenzene resin based on oxidized multi-walled carbon nanotubes. *Int J Modern Org Chem.* **2**(1), 67–80 (2013)
8. Fathy, M., et al.: Study the adsorption of sulfates by high cross-linked polystyrene divinylbenzene anion-exchange resin. *Appl. Water Sci.* **7**(1), 309–313 (2017)
9. El-Sayed, M., Ramzi, M., Hosny, R., Fathy, M., Moghny, T.A.: Breakthrough curves of oil adsorption on novel amorphous carbon thin film. *Water Sci. Technol.* **73**(10), 2361–2369 (2016)
10. Fathy, M., El-Sayed, M., Ramzi, M., Abdelraheem, O.H.: Adsorption separation of condensate oil from produced water using ACTF prepared of oil palm leaves by batch and fixed bed techniques. *Egypt. J. Pet.* (2017)
11. Wassel MA, Fathy M, Hosny R, Desouky AM and Mahmod AM. (2017) Study the removal of copper ions from textile effluent using cross linked chitosan. In 8 th International conferences of Textile Research Division
12. Magdy A. Wassel, M.F., R. Hosny, Desouky AM, Mahmod AM, and Abdelraheem OH (2018) "Evaluation of chromium (Cr III) adsorption using modified chitosan from different pH aqueous solutions". In 9th International Conference On CHEMICAL & Environ Eng
13. Fathy, M., Moghny, T.A., Abdou, M.M., Abdel-Hameed, A.-A., El-Bellihi, A.E.A.: Study the adsorption of Ca (II) and Mg (II) on high crosslinked polystyrene divinyl benzene resin. *Int. J. Modern Chem.* **7**(1), 36–44 (2015)
14. Mahmoud Fathy, T.A.M., Mousa, M.A., ElBellhi, A.-H.A.-A., Awadallah, A.E.: Sulfonated ion exchange polystyrene composite resin for calcium hardness removal. *Int. J. Emerg. Technol. Adv. Eng.* **5**(10), 20–29 (2015)
15. Ramzi M, et al. (2016) Breakthrough curves of oil adsorption on novel amorphous carbon thin film
16. Moghny, T.A., et al.: Preparation of sorbent materials for the removal of hardness and organic pollutants from water and wastewater. *World Acad. Sci. Eng. Technol. Int. J. Environ. Chem. Ecol. Geol. Geophys. Eng.* **11**(5), 461–468 (2017)
17. Fathy, M., Mousa, M.A., Moghny, T.A., Awadallah, A.E.: Characterization and evaluation of amorphous carbon thin film (ACTF) for sodium ion adsorption. *Appl. Water. Sci.* **7**(8), 4427–4435 (2017). <https://doi.org/10.1007/s13201-017-0588-3>
18. Ali, A., Bahadur Rahut, D., Behera, B.: Factors influencing farmers' adoption of energy-based water pumps and impacts on crop productivity and household income in Pakistan. *Renew. Sust. Energ. Rev.* **54**, 48–57 (2016)
19. Ali, M.E.A., et al.: Thin film composite membranes embedded with graphene oxide for water desalination. *Desalination.* **386**, 67–76 (2016)
20. Ammar, A.I., Kruse, S.E.: Resistivity soundings and VLF profiles for siting groundwater wells in a fractured basement aquifer in the Arabian Shield, Saudi Arabia. *J. Afr. Earth Sci.* **116**, 56–67 (2016)
21. Alvino, A., Barbieri, G.: Vegetables of temperate climates: leafy vegetables A2 - caballero, Benjamin. In: Finglas, P.M., Toldrá, F. (eds.) *Encyclopedia of Food and Health*, pp. 393–400. Academic Press, Oxford (2016)
22. Li, J., et al.: Nanoscale zero-valent iron particles modified on reduced graphene oxides using a plasma technique for Cd(II) removal. *J. Taiwan Inst. Chem. Eng.* **59**, 389–394 (2016)
23. Neelgund, G.M., Bliznyuk, V.N., Oki, A.: Photocatalytic activity and NIR laser response of polyaniline conjugated graphene nanocomposite prepared by a novel acid-less method. *Appl. Catal. B Environ.* **187**, 357–366 (2016)
24. Prince, J.A., et al.: Ultra-wetting graphene-based membrane. *J. Membr. Sci.* **500**, 76–85 (2016)
25. Sun, W., et al.: Synthesis of magnetic graphene nanocomposites decorated with ionic liquids for fast lead ion removal. *Int. J. Biol. Macromol.* **85**, 246–251 (2016)
26. Xu, K., et al.: Synthesis of highly stable graphene oxide membranes on polydopamine functionalized supports for seawater desalination. *Chem. Eng. Sci.* **146**, 159–165 (2016)
27. Xu, X., et al.: Design and fabrication of mesoporous graphene via carbothermal reaction for highly efficient capacitive deionization. *Electrochim. Acta.* **188**, 406–413 (2016)
28. Justh, N., et al.: Thermal analysis of the improved Hummers' synthesis of graphene oxide. *J. Therm. Anal. Calorim.* **131**(3), 2267–2272 (2018)
29. Zhu, Y., et al.: Monolithic supermacroporous hydrogel prepared from high internal phase emulsions (HIPEs) for fast removal of Cu<sup>2+</sup> and Pb<sup>2+</sup>. *Chem. Eng. J.* **284**, 422–430 (2016)
30. Alebeid, O.K., Zhao, T.: Review on: developing UV protection for cotton fabric. *J. Textile Instit.* **108**(12), 2027–2039 (2017)
31. Fathy, M., et al.: Cation exchange resin nanocomposites based on multi-walled carbon nanotubes. *Appl. Nanosci.* **4**(1), 103–112 (2014)
32. Afifi, A.M., et al.: Fabrication of aligned poly (L-lactide) fibers by electrospinning and drawing. *Macromol. Mater. Eng.* **294**(10), 658–665 (2009)

**Publisher's note** Springer Nature remains neutral with regard to jurisdictional claims in published maps and institutional affiliations.